Cork Open Research Archive
Cartlann Taighde Oscailte Chorcaí

UCC Library and UCC researchers have made this item openly available. Please let us know how this has helped you. Thanks!

Title	Exploratory study and application of the angular wavelet analysis for assessing the spatial distribution of breakdown spots in Pt/HfO2/Pt structures
Author(s)	Muñoz-Gorriz, J.; Monaghan, Scott; Cherkaoui, Karim; Suñé, Jordi; Hurley, Paul K.; Miranda, E.
Publication date	2017-12-05
Original citation	Muñoz-Gorriz, J., Monaghan, S., Cherkaoui, K., Suñé, J., Hurley, P. K. and Miranda, E. (2017) 'Exploratory study and application of the angular wavelet analysis for assessing the spatial distribution of breakdown spots in Pt/HfO2/Pt structures', Journal of Applied Physics, 122, 215304 (12pp). doi: 10.1063/1.5000004
Type of publication	Article (peer-reviewed)
Link to publisher's version	http://dx.doi.org/10.1063/1.5000004 Access to the full text of the published version may require a subscription.
Rights	**© 2017, the Authors. This article may be downloaded for personal use only. Any other use requires prior permission of the author and AIP Publishing. This article appeared as: Muñoz-Gorriz, J., Monaghan, S., Cherkaoui, K., Suñé, J., Hurley, P. K. and Miranda, E. (2017) 'Exploratory study and application of the angular wavelet analysis for assessing the spatial distribution of breakdown spots in Pt/HfO2/Pt structures', Journal of Applied Physics, 122, 215304 (12pp), doi: 10.1063/1.5000004, and may be found at: https://doi.org/10.1063/1.5000004**
Item downloaded from	http://hdl.handle.net/10468/13330

Downloaded on 2022-08-26T12:11:58Z

University College Cork, Ireland
Coláiste na hOllscoile Corcaigh

Exploratory Study and Application of the Angular Wavelet Analysis for Assessing the Spatial Distribution of Breakdown Spots in $Pt/HfO_2/Pt$ Structures

J. Muñoz-Gorriz[1], S. Monaghan[2], K. Cherkaoui[2], J. Suñé[1], P.K. Hurley[2], E. Miranda[1]

[1]Departament d'Enginyeria Electrònica, Universitat Autònoma de Barcelona, Spain

[2]Tyndall National Institute, University College Cork, Cork, Ireland

E-mail of corresponding author: jordi.munoz.gorriz@uab.cat

Abstract

The angular wavelet analysis is applied for assessing the spatial distribution of breakdown spots in $Pt/HfO_2/Pt$ capacitors with areas ranging from 10^4 to 10^5 μm^2. The breakdown spot lateral sizes are in the range from 1 to 3 µm and they appear distributed on the top metal electrode as a point pattern. The spots are generated by ramped and constant voltage stresses and are the consequence of microexplosions caused by the formation of shorts spanning the dielectric film. This kind of pattern was analyzed in the past using conventional spatial analysis tools such as intensity plots, distance histograms, pair correlation function, nearest neighbours, etc. Here we show that the wavelet analysis offers an alternative and complementary method for testing whether the failure site distribution departs or not from a complete spatial randomness (CSR) process in the angular domain. The effect of using different wavelet functions such as the Haar, Sine, French top hat, Mexican hat and Morlet as well as the roles played by the process intensity, location of the voltage probe and aspect ratio of the device are discussed.

Keywords: oxide breakdown, high-K, spatial statistics, wavelet analysis.

I. Introduction

One of the most studied issues in connection with the reliability of metal-insulator-metal (MIM) and metal-insulator-semiconductor (MIS) structures is the breakdown (BD) phenomenon of the oxide layer as it implies a fundamental change of the electrical properties of the devices [1]. Physically, this process consists in the generation of a defect percolation path inside the insulator and the formation of a short connecting the top and bottom electrodes allowing the unrestricted circulation of electrons [2]. If this process is not controlled, *i.e.* if the voltage or current is not limited by a series resistance or by the compliance of the experimental setup, the damage associated with the BD event is catastrophic and irreversible. The sudden flow of electrons through the formed conducting filament (CF) generates a huge increase of temperature due to Joule heating effects which ends with the local melting of the top metal layer [3]. The damage can extend to the bottom metal electrode as well. While for small area devices this highly energetic process completely destroys the top electrode, for large area devices it is possible to electrically detect a sequential BD process associated with the generation of distributed CFs over the whole device area [4]. As explained, each BD event leaves its mark on the top electrode due to the high thermal energy released, which can be confirmed by simple visual inspection through an optical microscope. The BD spots are crater-like structures so that they are referred to as hard BDs with lateral propagation [5]. If the size of the BD spots is neglected, the set of failure sites can be regarded from a mathematical perspective as a point pattern within an observation window.

In general, the study of the failure site distribution in MIS and MIM structures relies on electrical measurements such as ramped or constant current/voltage stresses applied to a large number of devices (with one BD event per device). Alternatively, it has been demonstrated that the methods of spatial statistics are appropriate too for investigating the distribution of BD spots in the case of multi-CF generation [6]. At the core of this research is assessing whether temporal or spatial correlations among the BD events occur or not. Experimental observations point out that the BD process in MIS and MIM devices is uncorrelated both in time and space [2]. The nearest neighbor distance histogram, the pair correlation function, and the Ripley's K function are frequently used first and second order estimators that provide information in that concern. In spatial statistics, data estimators are often compared with the corresponding theoretical values for a Poisson or complete spatial randomness (CSR) process [7]. Although deviations

can indicate that the studied distribution departs from CSR, the analysis is sometimes far from being conclusive. There is no single estimator able to provide the definitive solution to this problem since each estimator highlights a particular feature of the point pattern distribution. To overcome this limitation, a number of methods are often applied to the same data and the obtained results compared. As the generation of defects in an oxide layer is in principle a completely random process, an isotropic distribution of BD spots in the top metal electrode is expected to occur. However, deviations from CSR can happen as a consequence of some underlying properties of the generation process linked to the device fabrication method, oxide thickness nonuniformity, local variations of the permittivity value, edge effects, etc. [6,8-9]. The analysis of the distribution of BD spots gives insight about the quality of the oxide layer, *i.e* it can help to detect weak regions of the device. It is worth recalling also that, as in any statistical study, estimators can simply provide a summarized description of the observed data or, alternatively, they can be used for inferential purposes. In this latest case, a confidence band represents the uncertainty in an estimate of a curve based on limited data.

The angular wavelet analysis was developed by Rosenberg [10] and it is used to investigate the angular distribution of points in the plane from a global perspective, *i.e.* taking into account multiple focal points. The method is based on the wavelet transform, a mathematical tool frequently used for signal processing and data compression [11]. With this transform, data are weighted according to scaled and shifted wavelet functions. A wavelet is a wave-like shaped function whose integral over all x-values yields zero. There are many of such functions with different properties: continuous/discrete, orthogonal/biorthogonal, smooth/abrupt, etc. The wavelet transform and the angular wavelet analysis are mainly used for investigating geographical and ecological spatial data [11-12]. In this paper, the suitability of the angular wavelet analysis for assessing the BD spot distributions in MIM devices with high-k dielectric is explored. A preliminary study showed the adequacy of the method but did not deepen into the many factors that can affect the final outcome [13]. This paper is organized as follows: In Section II, the steps followed for the fabrication of the devices are described. The degradation conditions and the methodology used to analyze the results are reported. In Section III, the main mathematical features of the wavelet analysis are presented. The role played by the selected wavelet function is analyzed in Section IV. The method requires the definition of a focal window, a region located at the center of the observation window (device area) whose inner points are used as focal

points. It is shown that increasing or decreasing this area can significantly affect the obtained results. The computation time is also linked to this choice as well as with the selected wavelet function. This exploratory study of the method is fundamental to establish standard conditions for analyzing BD spot patterns. In Section V, different case studies are presented and discussed. First, devices with different number of BD spots are investigated. Second, the possible correlation between the location of the stress source and the spatial distribution of BD spots is investigated. Finally, the role played by the aspect ratio of the devices in the profile of the angular variance plot is reported.

II. Experimental details

The devices investigated in this work are Pt/HfO_2/Pt capacitors fabricated on top of n-type Si(100) substrates. First, a 200 nm thick thermal SiO_2 layer was grown on the Si substrate and a 200 nm thick Pt layer was deposited over the SiO_2 layer by electron-beam evaporation. A 30 nm-thick HfO_2 layer was then deposited by a Cambridge NanoTech Fiji atomic layer deposition (ALD) system using TEMAHf precursor and H_2O. After this, a 200 nm-thick Pt layer was deposited on top of the HfO_2 layer. Lithography and lift-off processes were used to form arrays of capacitors with different geometries. The access to the bottom Pt electrode was enabled via dry etching technique using a mask/resist process that removes the HfO_2 to the bottom Pt metal while at the same time protects the top Pt electrode of the patterned devices. The oxide layer extends 25 μm beyond the perimeter edge of the top metal electrode. The BD spots were generated using constant (9V for a maximum of 120 s) and ramped voltage stresses (from 0 V to 12 V). The bottom electrode was always grounded and the voltage was applied to the top electrode. The number of spots that can be generated depends both on the magnitude of the applied stress and the duration of the stress. There is always a limit in the number of spots that can be generated because of the increase of the potential drop across the series resistance as the degradation proceeds. Figure 1.a and 1.b show photographs of a pristine device and of an identical device after degradation, respectively. The BD spots appear as a point pattern distributed over the whole device area. Figure 1.c is a SEM image and shows a particular region of the top metal electrode of the device. The image shows that the size of the spots ranges from 1 to 3 μm. Figure 1.d corresponds to a detailed view of a particular failure site. Notice the crater-like

structure with the top metal layer upraised. Since the size of the spots is neglected, the only information required for the analysis is the location of the spots referred to the center of the structure (any other location is admitted). In what follows, BD spot patterns will be analyzed using the Spatstat [14] package for the R language and the PASSAGE2 software [15].

III. Brief introduction to the angular wavelet method

In this Section, a general description of the angular wavelet method is presented and the best conditions for assessing the failure site distribution in MIM devices established. The angular wavelet analysis is a method for analyzing anisotropy in point patterns. The focal window is defined as the region in which the focal points used for global analysis are located (see Fig. 2.a). The region around every focal point is divided into 1° angular sectors or quadrats, producing a total of 360 quadrats. As illustrated in Fig. 2.b, points in opposite quadrats are considered as a single data for calculating the density of points in a sector, making a total of 180 sector counts. This density is calculated as:

$$\rho(\alpha) = \frac{N(\alpha) + N(\alpha + 180°)}{A(\alpha) + A(\alpha + 180°)} \tag{1}$$

where α is the angular direction of a merged sector, and N and A are the number of points and area of a 1° sector, respectively. Notice that α ranges from 0° to 180°. As shown in Fig. 2.c, these sectors form a circular transect, the last and the first sectors are assumed to be adjacent. The wavelet transform is then applied to this transect $\rho(\alpha)$. In the wavelet transform, a wavelet function (w) is shifted to a given location of the experimental data (α_i) and scaled to a given size (b_k) (see Fig. 3). This scaling process determines the range of the data sequence that will be accounted for by the transform. The wavelet transform (W) at the position α_i for scale b_k is expressed as:

$$W(b_k, \alpha_i) = \frac{1}{b_k} \sum_{j=1}^{n} \rho(\alpha_j) \times w\left(\frac{\alpha_j - \alpha_i}{b_k}\right) \tag{2}$$

where $\rho(\alpha_i)$ is the data value at the location α_i and n is the number of observations along the transect. When good matching between the experimental value and the scaled wavelet function is achieved, the wavelet transform at that position is high. Otherwise, for a poor matching, a low value is obtained (Fig. 3). Notice that (2) yields a single

value for each position and scale. In this method, the variance for a given sector α_i evaluated at different scales (b_k) is calculated as:

$$P(\alpha_i) = \frac{1}{m}\sum_{k=1}^{m} W^2(b_k, \alpha_i) \tag{3}$$

Expression (3) corresponds to the average of the squared wavelet transform over all possible scales (m is the total number of considered scales). In the angular wavelet method, the scale (b_k) ranges from 1° to 45° in steps of 1°. Taking into account all the focal points within the focal window, the average variance reads:

$$P_t(\alpha_i) = \frac{1}{l}\sum_{l=1}^{f} P_l(\alpha_i) \tag{4}$$

where f is the number of focal points. In order to assess the angular distribution of points, a comparison is made between the experimental variance and the prediction corresponding to a CSR process (ideally a circle centered at the origin of coordinates). In practice, the CSR variance plot is obtained by randomizing the location of all the data points in the observation window r times. These r Poisson distributions are analyzed using the wavelet analysis and the confidence band calculated. The confidence band is used to evaluate in what extent the experimental data shows anisotropy. In case that the point pattern does not follow a Poisson distribution, the experimental variance can exhibit one or several peaks exceeding the confidence band limit. The presence of such peaks might indicate an accumulation of spots in a particular direction of the pattern. Here, we have considered a 95% confidence band which is obtained after randomizing the experimental data 50 times.

An alternative approach to the wavelet method consists in calculating the angular variance of the experimental data taking into account solely the density of points at each angular position (angular bins) using a central focal point. This method can be used to detect accumulation of spots in particular directions. However, despite this approach seems more simple and straightforward than the angular wavelet analysis described above, it only involves a single focal point, *i.e.* the center of the structure. This is at variance with the spirit of spatial methods which does not rely on a particular point location but on a global analysis. However, a focal window could be defined for obtaining an angular histogram but in this case the results would be still limited to a single bin size. Recall that the wavelet method is a multiscale approach.

IV. Exploratory analysis

In this Section, the angular wavelet analysis is applied to different case studies and the obtained results discussed. A number of issues such as the effects of the wavelet type, focal window, and computational time are investigated. This exploratory analysis is an essential prerequisite to the application of the method since it provides the clues for the understanding of the particular features of the estimates. This Section is also intended to serve as a guide for similar studies other than the one reported here. Distances are normalized to the nominal lateral sizes of the devices and angles are measured with respect to the horizontal. For the sake of completeness, the Kolmogorov-Smirnov (*K-S*) test and the pair correlation function (g) are also investigated. The *K-S* test is a statistical method in which the empirical cumulative distribution function (CDF) is compared with a reference CDF in order to assess or reject the null hypothesis. In spatial statistics, the empirical CDF for the location of the spots along an axis (x or y coordinate) is compared with the CDF for a CSR distribution. The null hypothesis (CSR distribution) is rejected when the $p\text{-}value \leq 0.05$. The $g(r)$ function is related to the probability of finding a point at a distance r from another point. The expected value for a CSR process is $g(r)=1$. This result is compared with the experimental $g(r)$.

a. Application of conventional tests

The BD spot distribution in a square capacitor with area 750 µm x 750 µm (Fig. 4.a) will be studied first. 343 BD spots were generated by means of a constant voltage stress (9 V for 120 s). The process intensity is $\lambda=6.1\cdot10^{-4}$ spots/µm^2. Figure 4.b shows the locations of the BD spots used for computation. Figures 4.c and 4.d show the pair correlation function g as a function of the generic distance r and the results of the Kolmogorov-Smirnov (*K-S*) test for the x and y coordinates of the points, respectively. These are conventional tools of spatial statistics. Figure 4.c shows that the experimental g value fluctuates around the unity which corresponds to a CSR process. The plot also includes the 95% confidence band (shaded region). The obtained result indicates that the distribution of points is compatible with a homogenous Poisson process for interpoint distances in the range $r<0.25$. Nevertheless, the *K-S* test (see Fig. 4.d) exhibits a remarkable deviation from CSR in the x direction. A good matching with a Poisson process is just observed in the y direction, as demonstrated by the high p-value obtained. For the x direction the *null* hypothesis can be rejected (low p-value), as a large mismatch between the experimental and the theoretical cumulative distribution

functions (CDF) is detected. This case study illustrates the difficulties associated with considering a single estimator for the analysis of point patterns.

b. *Role played by the wavelet function*

The PASSAGE2 software offers five types of wavelets for angular analysis. The Haar and the French top hat are discrete wavelets, whereas the Sine and the Mexican hat are their continuous form, respectively. Additionally, a more complex wavelet form, the Morlet, is also available. The different wavelet basis and their mathematical expressions are described in Fig. 5. Figures 6.a-e show the results of applying the angular wavelet analysis to the device shown in Fig. 4.a. Each figure corresponds to a different wavelet basis (see the insets). The 95% confidence bands are also included in the plots. For most wavelet basis (Fig. 6.a-c), a peak in the experimental variance curve is observed at approximately 90º. The peak is somewhat above the confidence band which suggests certain degree of anisotropy. Notice that just in the case of the Morlet wavelet basis (Fig. 6.e), the experimental variance is below the confidence band for all possible directions. The appearance of this peak can be ascribed to the accumulation of points in the x direction (Fig. 4.d). This feature was already detected by the *K-S* test. It is worth pointing out that despite the fact the accumulation of spots is detected by the angular wavelet analysis, the observed peaks are not high enough to fully reject the *null* hypothesis. In order to better show the effect of each wavelet basis, the experimental variances are represented all together in a single plot (see Fig. 6.f). It can be observed that the Sine and the Mexican hat wavelets show the lowest variance values, and that these values increase when their discrete form of the wavelet is used. Not only the variance increases but also the sensitivity for detecting accumulation of spots, being the French top hat the wavelet that shows the highest contrast in the whole angular range. On the other hand, despite the Morlet wavelet displays the lower contrast, it also shows the higher variance value in all directions.

c. *Effect of the analysis window*

In the angular wavelet analysis, the angular density of points is calculated by dividing the space in regular angular sectors around specific points. The selection of these focal points follows a criterion which consists in defining a small square area in the center of the structure with the edges as far as possible from the whole observation window (area of the device). This is necessary to avoid corner effects in the angular

distributions [10]. The focal window is calculated in PASSAGE2 as a percentage of the observation window. For instance, a 20% focal window corresponds to a square area 5 times smaller than the total area covered by the point pattern. In order to study the effect of the focal point locations, the point pattern illustrated in Fig. 4.b was analyzed using different focal window sizes. Fig. 7.a-e show the different angular wavelet analysis results with their corresponding 95% confidence bands. The dotted square indicates the focal window. Because of its high contrast, the French top hat wavelet was used for computation. It can be seen that the shape of the confidence band strongly depends on the size of the focal window. For small focal windows (Fig. 7.a-b), high variance peaks appear along their diagonals. As the focal window size is increased, the peaks disappear, after which new ones develop perpendicularly to the device sides (Fig. 7.d-e). This modification of the confidence band is attributed to the sensitivity of the analysis as a function of the focal window size in comparison with the total observation window. Importantly, for the 20% focal window (Fig. 7.c), the confidence band is almost isotropic which discards any edge effect. Now, if we pay attention to the experimental angular distribution, a small peak rises above the confidence band around 90º which closely agrees with the results discussed earlier. Notice that the shape of the experimental variance is also affected by the size of the focal window as it happens for the confidence band (Fig. 7.f). However, it can be seen that the experimental variance does not increase in the 0º/180º direction as could be expected. The variance increases in the direction where the peak appears, in the 90º/270º direction. This suggests that a comparison between the variances associated with the confidence band and experimental data is fundamental to assess the isotropy of the point pattern. However, in these case studies (Fig. 7.a-e), the *null* hypothesis cannot be completely rejected since the differences between the experimental variances and the confidence bands are relatively small.

d. Computation time

In the field of data analysis not only it is important to have accurate estimators but also it is imperative to know the time required to achieve such results. Normally the time involved is not significant when a few points are considered. On the contrary, for a large point pattern the computational time can be a key factor for deciding which method will be used to treat data. In the angular wavelet analysis it is obvious that the higher the density of points is, the higher the time required to perform calculations

essentially because of the increased number of focal points. Importantly, the analysis time also depends on the wavelet function considered. In order to study the time consumption as a function of the number of points and wavelet basis, point distributions were mathematically generated in a 1x1 area according to a random process. For a fixed number of points (binomial point pattern), a single distribution was generated and analyzed with the different wavelet functions. A 20% focal window was used to carry out this mathematical experiment. Figure 8 shows the normalized time required to complete the analysis. The reference time is computed for a Haar wavelet and a realization with 100 points (t_0=1.4 s). The Haar wavelet exhibits the lowest computation time. As expected, the time does not follow a linear progression with the number of points. This happens because the number of focal points also increases with the number of points. Interestingly, the time required for the analysis also increases with the complexity of the wavelet considered. Discrete wavelets, such as the Haar and French top hat are lower time consuming than their continuous counterparts, the Sine and the Mexican hat, respectively, being faster the Sine than the French top hat. A wide time gap is also observed between the French and the Mexican hat due to the increase in complexity. In addition, as expected, the Morlet wavelet requires the largest computation times.

IV. Further experimental results and discussion

Once the exploratory analysis is carried out, the next step is applying the method to different distributions of BD spots and interpreting the results. In this Section, three case studies are reported. In the first case, the devices under investigation show multi-CF generation (different number of spots) obtained after applying medium to severe electrical stress. In the second case, a severely damaged device is investigated but, in this case, the location of the source of degradation (voltage probe) is taken into account. In the third case study, the effect of the aspect ratio of the device on the angular variance profile obtained by PASSAGE2 is investigated. According to what was discussed in previous Sections, the angular wavelet analysis will be performed using a 20% focal window and the French top hat wavelet. As before, the 95% confidence band is calculated from the complete randomization of the spot locations.

a. Role played by the process intensity

Figure 9.a shows a photograph of a square capacitor with area 750 μm x 750 μm. 275 BD spots were counted (see Fig. 9.b) which corresponds to an intensity $\lambda=4.89\cdot10^{-4}$ spots/μm^2. The pair correlation function g fluctuates around the unity value which indicates that the point pattern is consistent with a CSR process (see Fig. 9.c). As shown in Fig. 9.d, this observation is also supported by the angular wavelet method. Although some deviations from isotropy are detected, the 95% confidence band is always above the experimental variance curve for all possible directions. Figure 10 shows an example in which the number of BD spots is remarkably larger. In this case, 3603 BD spots were counted which for a device with area 500 μm x 500 μm yields a process with intensity $\lambda=1.44\cdot10^{-2}$ spots/μm^2. This is two orders of magnitude higher than the previous example. The location of all the failure sites analyzed is depicted in Fig. 10.b. A preliminary analysis using g (see Fig. 10.c) supports the hypothesis of a CSR process for distances in the range $r<0.25$. Notice that the confidence band is narrower than in the previous case as expected for a larger number of observations. Again, the angular wavelet analysis clearly supports the isotropy of the point distribution (Fig. 10.d). In this case, both the 95% confidence band as well as the experimental variance are almost circular and well distant apart.

b. Presence of the voltage probe

A question one can rise is whether it is possible or not to correlate the damage distribution over the structure with the location of the source of degradation, *i.e.* the voltage probe. This is different from the previous cases, in which the location of the probe was *a priori* unknown. The analysis is still global so that the voltage probe will not be used as a focal point. A local analysis of this problem can be found in [6]. In the experiments studied in this Section, the devices have an area 200 μm x 200 μm. However, the number of BD spots considered is radically different. In Fig. 11.a, a device with 124 BD spots and a process intensity $\lambda=3.1\cdot10^{-3}$ spots/μm^2 is shown. The locations of the failure sites are illustrated in Fig. 11.b. A preliminary analysis reveals that the generation of spots is consistent with a Poisson process as the $g=1$ value is within the confidence band limits (see Fig. 11.c). However, a slight deviation from a CSR process is detected in the x direction of the angular variance plot (Fig. 11.d). This is consistent with the distribution of points illustrated in Fig. 11.b. Notice also that there is a small peak pointing out toward the voltage probe location but the peak is so close to the confidence band that the result is not conclusive. In a second example (see Fig.

12.a), the device exhibits 456 BD spots corresponding to a process intensity $\lambda=11.4\cdot10^{-3}$ spots/μm^2. Figure 12.b shows the locations of all the failure sites analyzed. The pair correlation function *g* (Fig. 12.c) suggests that the generation of BD spots is consistent with a homogenous Poisson process (shaded area). Nevertheless, the experimental *g* curve is slightly above unity which indicates a larger density of points than that expected for a CSR process. In this case, the angular wavelet analysis (Fig. 12.d) reveals an accumulation of spots in the 160º direction. This result neither supports the CSR hypothesis nor the connection of the point pattern anisotropy with the voltage probe location. These two examples demonstrate the difficulties involved in trying to establish any link with the source of degradation when the number of spots is relatively low. In a third example, a device with a much higher number of BD spots (2055) and with severe signs of degradation is investigated (Fig. 13.a). The corresponding process intensity is $\lambda=51.37\cdot10^{-3}$ spots/μm^2. The spots were generated using constant voltage stress (9 V for 180 s). Notice that a dark region coming out from the voltage probe and pointing out toward the center of the device is clearly visible (Fig. 13.a). This burned area is a consequence of the current flow distribution over the top electrode. This dark region seems to indicate that the voltage probe could have some influence in the spot generation that should be detected by the angular wavelet method. Figure 13.b illustrates the locations of the BD spots. Figure 13.c shows the experimental pair correlation function *g* and the expected value for a CSR distribution. According to these results the BD spot distribution seems to be consistent with a Poisson process yet some deviation can be observed. The angular plot (Fig. 13.d) confirms that the distribution is isotropic, rejecting again the possible implication of the probe location in the distribution of the BD spots. These results are *a priori* at variance with what is observed in Fig. 13.a. The SEM image in Fig. 14 illustrates the origin of this discrepancy. Beyond the kind of spots that are under investigation (crater-like), a large amount of small defects or product debris associated with the microexplosions are detected on the top metal electrode (see the arrows). The size of these small points is in the range from 10nm to 1μm and they form the darker region (Fig. 13.a). In all the previous examples, only the large BD spots, *i.e.* those strictly related to the microexplosions were counted. This is the reason why no influence of the voltage probe is detected in the final distribution of failure sites using the standard analysis.

Nevertheless, it is worth investigating whether any kind of anisotropy can be detected by modifying the original focal window. The results are reported in Fig. 15.

The confidence bands and the experimental results are illustrated in Figs. 15.a and 15.b, respectively. As it can be seen, lobes in the 45º and 135º directions appear as the size of the focal window is reduced. Despite the fact the experimental angular variance is below the confidence band for focal windows smaller than 20%, it can be observed that the profile of the experimental curve becomes asymmetric. A slight anisotropy is detected by the angular wavelet method in the direction of the voltage probe when the focal window is reduced to 5%. In this case, not only the *null* hypothesis is rejected, as it has been previously discussed, but also indicates that the voltage probe should have some influence in the generation of BD spots. This happens because the voltage probe is located in the same direction in which the sensitivity of the method increases, making easier the detection of effects associated with the voltage probe location. Once again, the method reveals its usefulness but at the same time reflects that a fine tunning of the parameters of analysis is strongly required.

c. Effect of the aspect ratio of the MIM structure

In previous Sections, the distribution of failure sites in square area devices was investigated. Here, the role played by the aspect ratio of the structures in the angular plot will be discussed. For that aim, two devices with different area and shape will be studied. As in the previous examples, a 20% focal window, the French top hat wavelet and 50 iterations for the 95% confidence band are assumed. Figure 16.a shows a photograph of the device. 138 BD spots were counted in an area 1250 µm x 800 µm which corresponds to a process with intensity $\lambda=1.38\cdot10^{-4}$ spots/µm^2. The locations of the BD spots after normalization are illustrated in Fig. 16.b. The pair correlation function g is represented in Fig. 16.c together with its 95% confidence band. Notice that the experimental g curve fluctuates around the unity value indicating a CSR process. This is in agreement with the results obtained by angular wavelet analysis (Fig. 16.d), as the experimental variance does not exceed the confidence band. Notice that both curves exhibit higher variance values as the angle of analysis approaches 90º. Notice that the overall variance plot is radically different from what was observed in previous cases for square area devices. In the second example, the area of the device is 650 µm x 150 µm (Fig. 17.a). A total of 583 BD spots were counted (Fig. 17.b) corresponding to a process intensity $\lambda=5.98\cdot10^{-3}$ spots/µm^2. Notice that this device is larger than the previous one and that the aspect ratio is also different. Again the experimental g value fluctuates around unity as expected for a CSR process (Fig. 17.c). Moreover, the angular wavelet

method (Fig. 17.d) shows no accumulation effects of spots in any particular direction. It is observed that the experimental variance curve as well as the confidence band curve shrinks at 0º and 180º. However, the narrowing effect in this case is stronger than that observed before (Fig. 16.d). It is clear that the main changes in the variance occur in the direction in which the lateral dimension of the device increases. Importantly, the dimensions of the observation window also affect the values and shape of the angular variance plot. This reinforces the importance of calculating and comparing the confidence band in order to make inferences about the BD spot distribution in MIM devices.

V. Conclusions

In this paper the application of the angular wavelet method for assessing the generation of BD spots on the top metal electrode of large area MIM devices was investigated. The main characteristics of the method were reported as well as how the results are affected by the chosen wavelet function, focal window, number of points, etc. From this study, it was found that not only it is important to consider the values of experimental angular variance plot but also the associated confidence band. The French top hat wavelet and a 20% focal window were found to be the optimal combination for achieving the best outcome from the method though some variations may be required in particular situations. Using these values, BD spot distributions obtained under different conditions were investigated. The analysis performed on square devices revealed isotropic distributions of BD spots as expected for Poisson point processes. Although in most of the cases CSR was found, the angular wavelet method needs to be complemented with other second order estimates such as the pair correlation function. It was shown that under standard conditions the method is not capable of detecting the effect of the voltage probe location on the failure site distribution. However, it was possible to detect a correlation between the voltage probe and the generation of BD spots when small focal windows were taken into account. From the analysis of rectangular area devices it was observed how their aspect ratios significantly modify the angular plot. Finally, it is worth mentioning that the angular wavelet analysis could be particularly relevant for the reliability assessment of large area electron devices other

than the one investigated here with similar marks or point defects scattered over their surfaces.

Acknowledgement

This work was supported in part by the ENIAC Joint Undertaking under the PANACHE EU Project and the DURSI through the Generalitat de Catalunya under Grant 2014SGR384. E. Miranda acknowledges the support from the EU Ascent Project (Tyndall National Institute-Ref.030).

References

[1] A. Oates, in IEDM Tech. Dig., pp. 923-926, 2003.

[2] E.Y Wu, J.H Stathis, L.-K. Han, Semicond. Sci. Technol., vol. 15, no. 5, pp. 425, 2000.

[3] E. Miranda, M. Ricio, G. De Falco, J. Blasco, J. Suñé, A. Irace, J. Appl. Phys., vol. 115, pp. 174502-1/6, 2014.

[4] S. Lombardo, J.H. Stathis, B.P. Linder, K.L. Pey, F. Palumbo, C.H. Tung, J. Appl. Phys., vol. 98, no.12, pp. 121301-1/36, 2005.

[5] S. Chatterjee, S. Chatterjee, Y. Kuo, J. Lu, J.-Y. Tewg, P. Majhi, Microelectron. Reliab., vol 46, pp. 69-76, 2006.

[6] X.S. Mas, S. Monaghan, P. K. Hurley, J. Suñé, E. Miranda, IEEE Trans. Device Mater. Rel., vol. 14, no. 4, pp. 1080-1090, 2014.

[7] J. Illian, A. Penttinen, H. Stoyan, D. Stoyan, *"The homogenous Poisson point process in Statistical analysis and modelling of spatial point patterns"*, S. Senn, M. Scott, V. Barnett, Ed. John Wiley & Sons: England , pp. 57-97, 2008.

[8] Y.-L. Li, Zs. Tökei, Ph. Roussel, G. Groeseneken, K. Maex, Microeletron. Reliab., vol. 45, pp 1299-1304, 2005.

[9] E. Miranda, D. Jiménez, J. Suñé, E. O'Connor, S. Monaghan, I. Povey, K. Cherkaoui, P.K. Hurley, J. Vavuum Sci. Technol. B, Microelectron. Nanomeer Struct., vol. 31, no 1, pp. 01A107-1/6, 2013.

[10] M.S. Rosenberg, J. Veg. Sci., vol. 15, pp. 277-284, 2004.

[11] C.K. Chui, Academic Press, vol. 1, 1992.

[12] M.R.T. Dale, M. Mah, J. Veg. Sci., vol. 9, pp. 805-814, 1998.

[13] J. Muñoz-Gorrriz, S. Monaghan, K. Cherkaoui, J. Suñé, P.K. Hurley, E. Miranda, Microelectron. Eng., vol. 178, pp. 10-16, 2017.

[14] A. Baddeley, R. turner, J. Stat. Softw., vol. 12, pp. 1-42, 2005.

[15] M.S. Rosenberg, C. D. Anderson, Methods Ecol. Evol., vol. 2, no 3, pp. 229-232, 2011.

Figure captions

1) Photograph of (a) pristine device and (b) stressed device. (c) SEM image of the top electrode after degradation. (d) Detailed SEM image of a typical BD spot.

2) (a) Selection of focal points in a point pattern in the center of the distribution. (b) Distribution of angular sectors for a given focal point. (c) Transect generated from sectors indicating circularity.

3) Schematic of a sequence of experimental data ($\rho(\alpha_j)$) and corresponding wavelet matching process. α_i is the position where the transform is applied and b_k is the scale of the wavelet template. When the wavelet function matches the data sequence, a high wavelet transform value is obtained (e.g. left window). For a poor match, a small value of wavelet transform is obtained (e.g. right window).

4) (a) Photograph of a multiple BD spot distribution in square area capacitor with size 750 µm x 750 µm. (b) Location of points in the capacitor area. (c) Pair correlation function g for the experimental data and for a CSR process. (d) Kolmogorov-Smirnov (*K-S*) test for the x and y direction and for a CSR process. The p-value obtained from the *K-S* test for each direction is indicated.

5) Available wavelet functions in PASSAGE2 to perform the angular wavelet analysis. The scheme shows their mathematical definitions as well as their schematic representations.

6) Angular wavelet analysis results obtained from the point pattern shown in Fig. 4.b with a 20% focal window and using (a) Haar, (b) Sine, (c) French top hat, (d) Mexican hat and (e) Morlet wavelet function. The 95% confidence band is obtained after randomizing the experimental data 50 times. (f) Representation of all the experimental data results shown in Figs. 6.a-e.

7) Angular wavelet analysis results obtained from the point pattern shown in the Fig. 4.b using the French top hat wavelet function with (a) a 5%, (b) a 10%, (c) a 20%, (d) a 30% and (e) a 40% focal windows. The 95% confidence band is obtained after

randomizing the experimental data 50 times. (f) Representation of all the experimental data results shown in Figs. 7.a-e. The arrows point out the changes observed in the experimental curves when the focal window is increased.

8) Normalized time required to complete a wavelet analysis as a function of the number of total points in a 1x1 area. The computation does not include the calculus of the confidence band. The points have been mathematically generated following a binomial distribution (fixed number of points). The time required for different wavelet functions are shown. A 20% focal window was used in all the cases. The reference time (t_0=1.4 s) is the time required by the fastest analysis performed (Haar wavelet and 100 points).

9) (a) Photograph of a multiple BD spot distribution in a square area capacitor with size 750 µm x 750 µm. (b) Location of the spots in the capacitor area. The dotted square indicates the 20% focal window used to determine the focal points. (c) Pair correlation function *g* for the experimental data and for a CSR process. (d) Angular wavelet analysis using a 20% focal window and the French top hat wavelet function. The 95% confidence band is obtained after randomizing the experimental data 50 times.

10) (a) Photograph of a multiple BD spot distribution in square area capacitor with size 500 µm x 500 µm. (b) Location of the spots in the capacitor area. The dotted square indicates the 20% focal window used to determine the focal points. (c) Pair correlation function *g* for the experimental data and for a CSR process. (d) Angular wavelet analysis using a 20% focal window and the French top hat wavelet function.

11) (a) Photograph of a multiple BD spot distribution in square area capacitor with size 200 µm x 200 µm. The position of the voltage probe is known (dark area at the corner of the device). (b) Location of all 124 BD spots in the capacitor area. The dotted square indicates the 20% focal window used to determine the focal points. (c) Pair correlation function *g* for the experimental data and for a CSR process. (d) Angular wavelet analysis using a 20% focal window and the French top hat wavelet function.

12) (a) Photograph of a multiple BD spot distribution in square area capacitor with size 200 µm x 200 µm. (b) Location of all 456 BD spots in the capacitor area. The dotted square indicates the 20% focal window used to determine the focal points. (c) Pair correlation function *g* for the experimental data and for a CSR process. (d) Angular wavelet analysis using a 20% focal window and the French top hat wavelet function.

13) (a) Photograph of a multiple BD spot distribution in square area capacitor with size 200 µm x 200 µm dimensions. (b) Location of all 2055 BD spots in the capacitor area. The dotted square indicates the 20% focal window used to determine the focal points. (c) Pair correlation function *g* for the experimental data and for a CSR process. (d) Angular wavelet analysis using a 20% focal window and the French top hat wavelet function.

14) SEM image of the sample shown in the Fig. 13.a. A typical BD spot can be observed in the center of the image and smaller defects are pointed out with arrows. These defects are observed in the optical image (Fig. 13.a) as a dark region coming out from the voltage probe position. The locations of these defects were not taken into account in the angular wavelet analysis.

15) (a) 95% confidence band and (b) angular wavelet analysis for the point pattern shown in the Fig. 12.b using different focal windows sizes. The 95% confidence band is obtained after randomizing the experimental data 50 times.

16) (a) Photograph of a multiple BD spot distribution in a rectangular area capacitor with size 1250 µm x 800 µm. (b) Location of the spots in the capacitor area. The dotted square indicates the 20% focal window. (c) Pair correlation function *g* for the experimental data and for a CSR process. (d) Angular wavelet analysis using a 20% focal window and the French top hat wavelet function.

17) (a) Multiple BD spot distribution in rectangular area capacitor with size 650 µm x 150 µm. (b) Location of the spots in the capacitor area. The dotted square indicates the 20% focal window. (c) Pair correlation function *g* for the experimental data and

for a CSR process. (d) Angular wavelet analysis using a 20% focal window and the French top hat wavelet function.

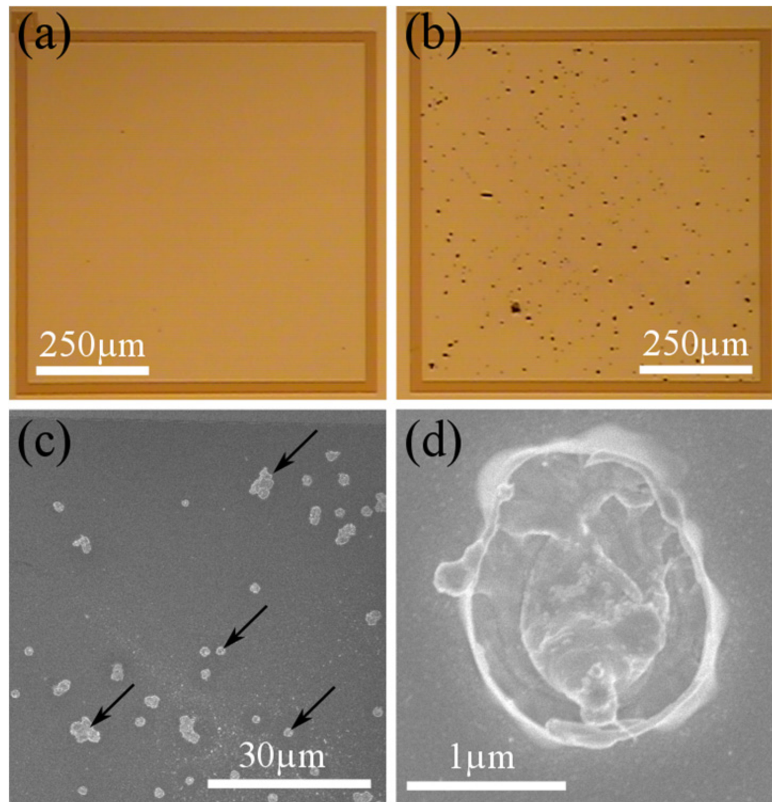

FIGURE 1

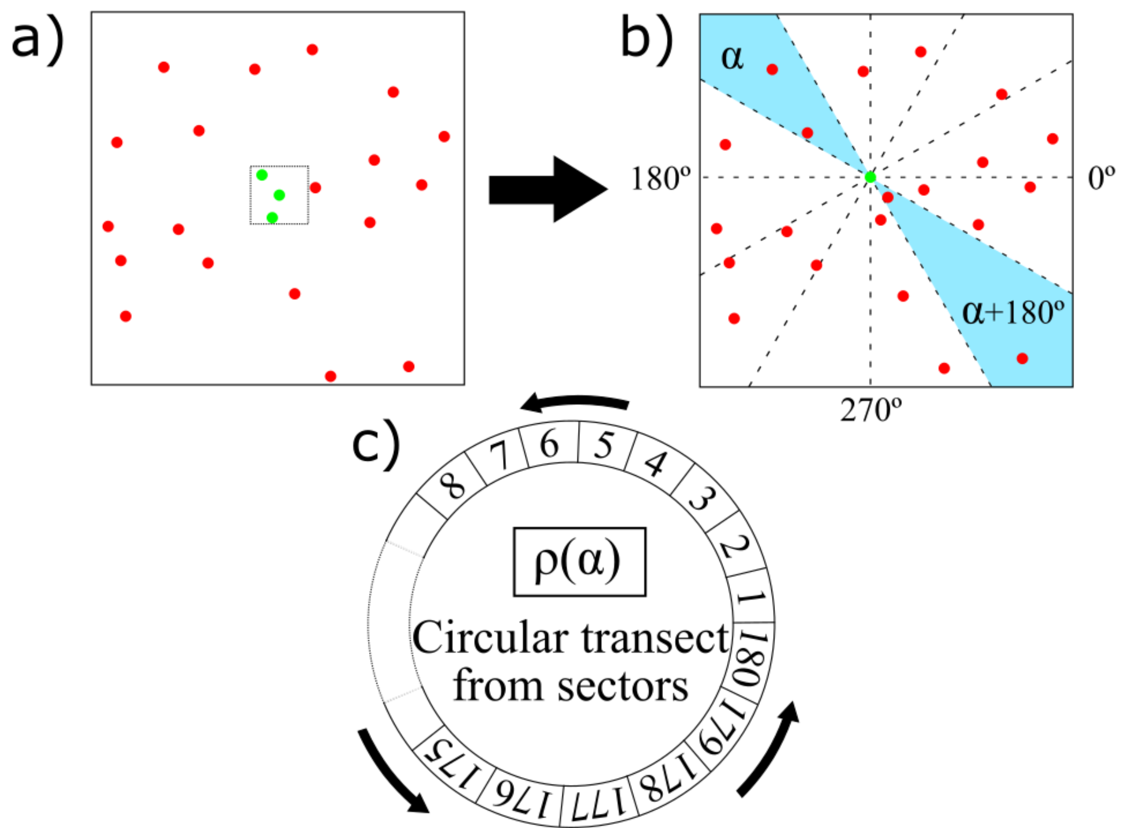

FIGURE 2

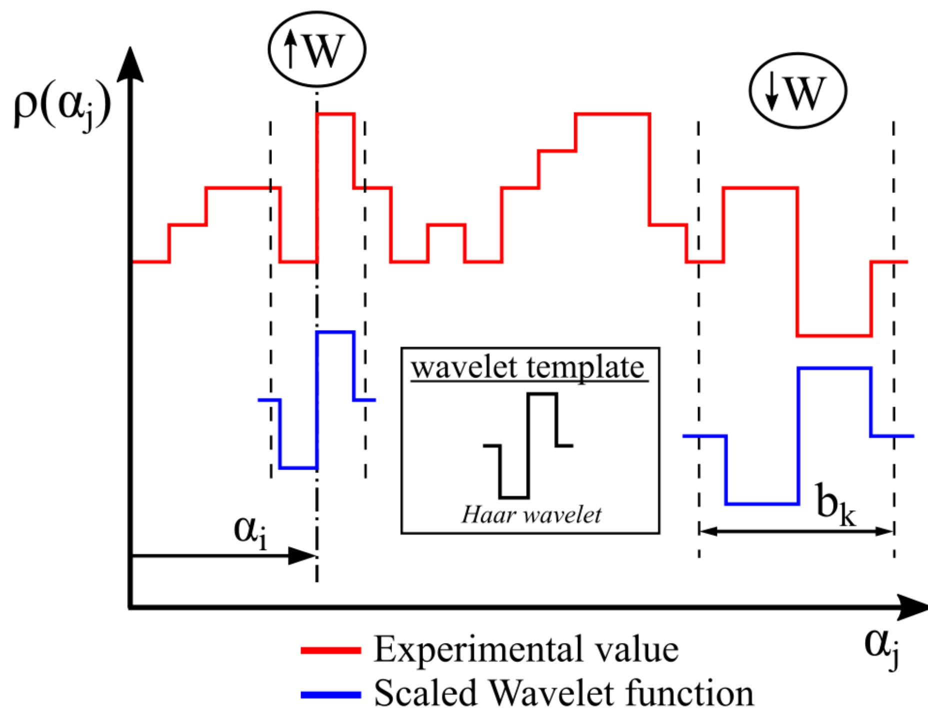

FIGURE 3

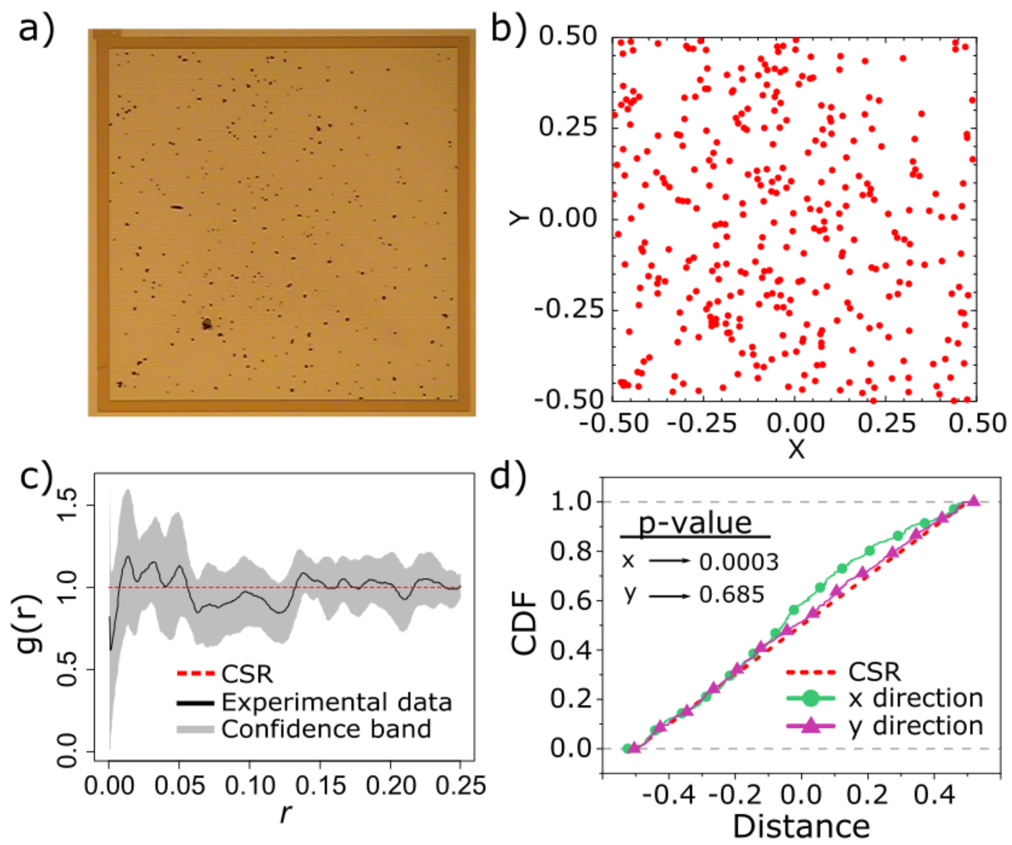

FIGURE 4

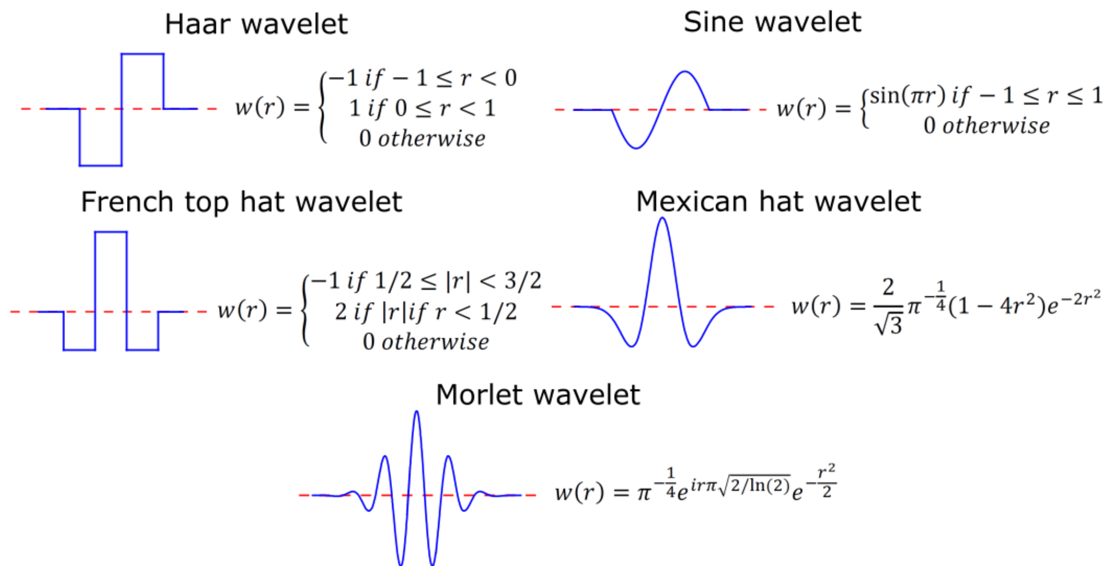

FIGURE 5

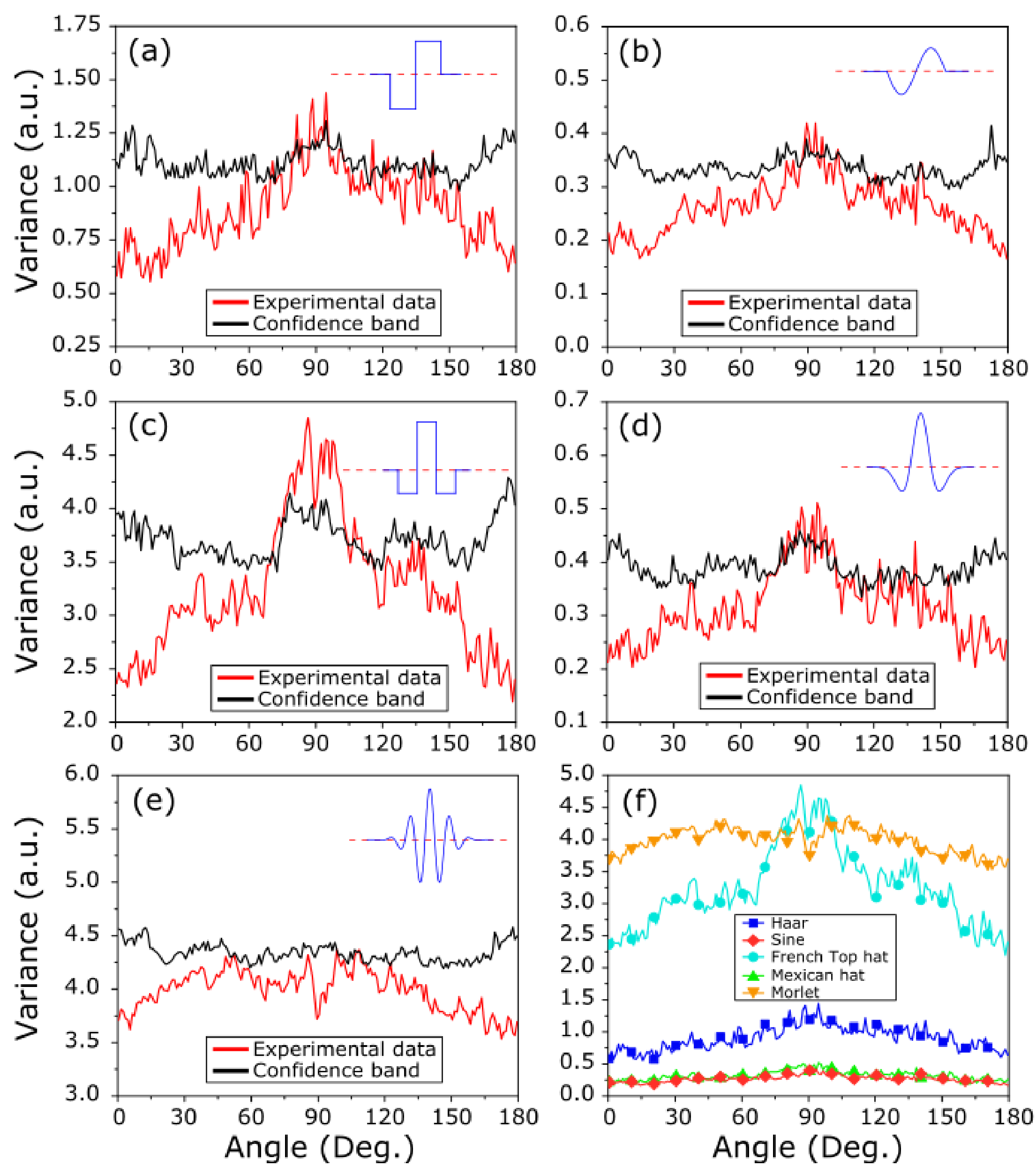

FIGURE 6

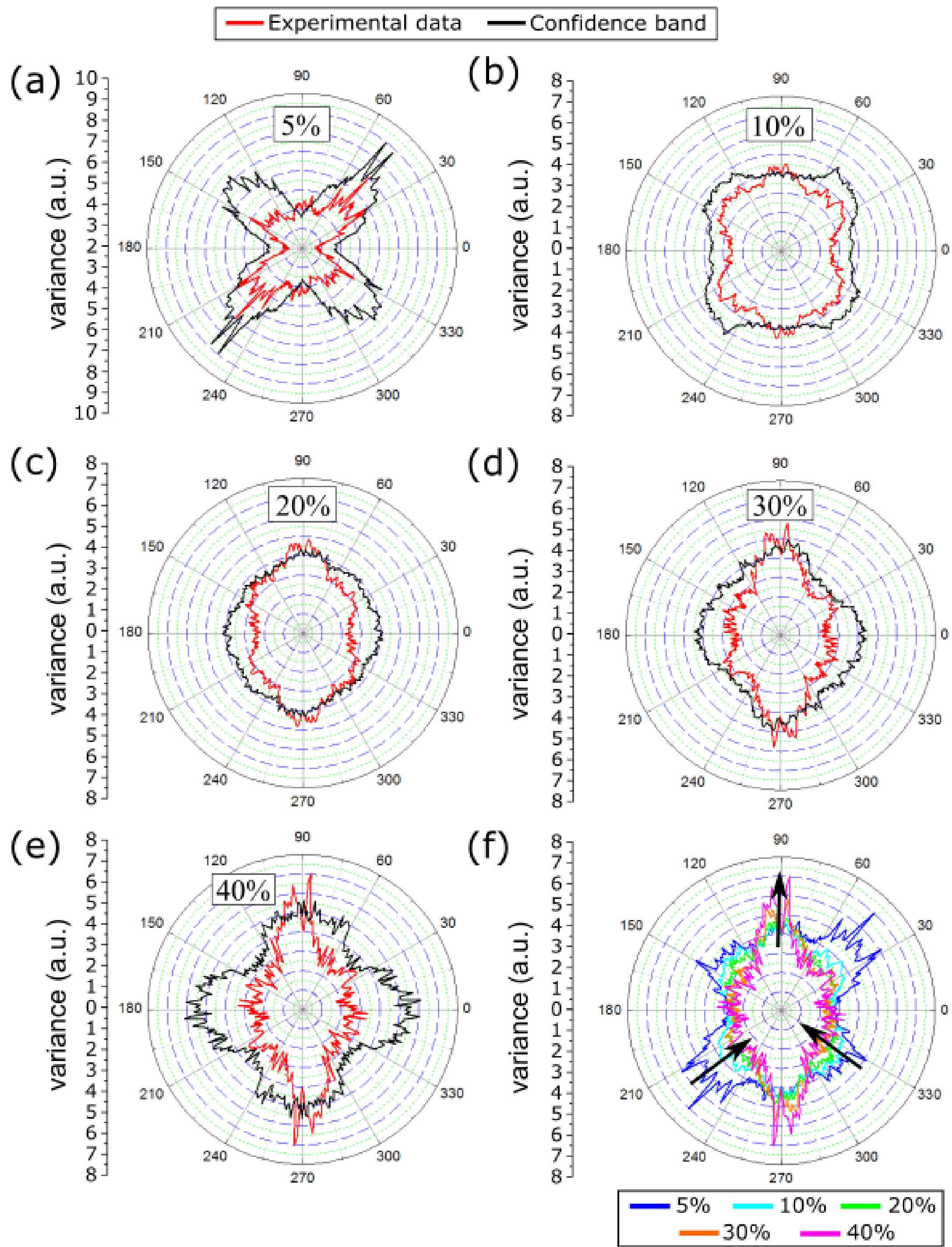

FIGURE 7

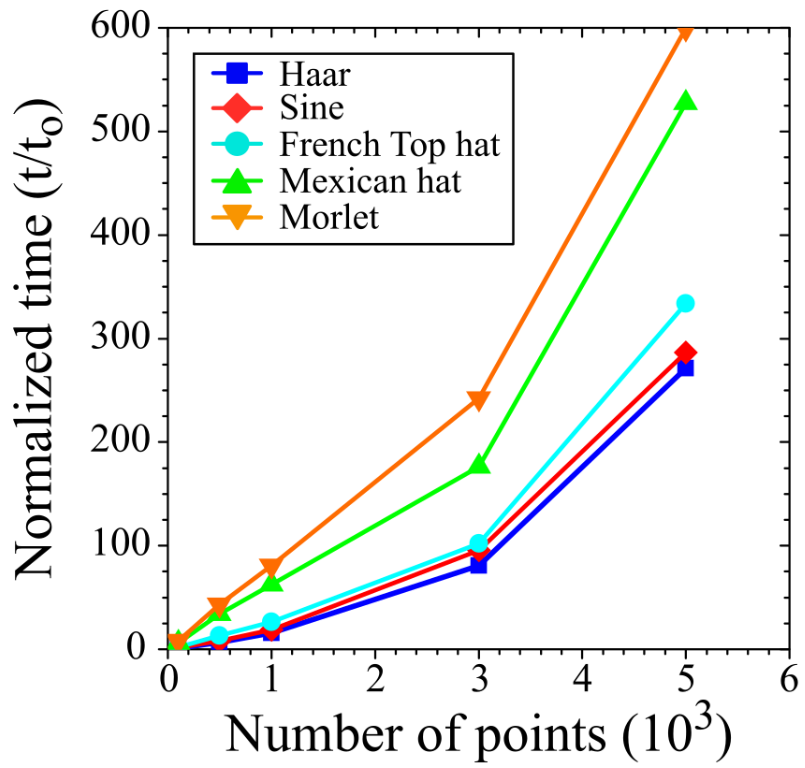

FIGURE 8

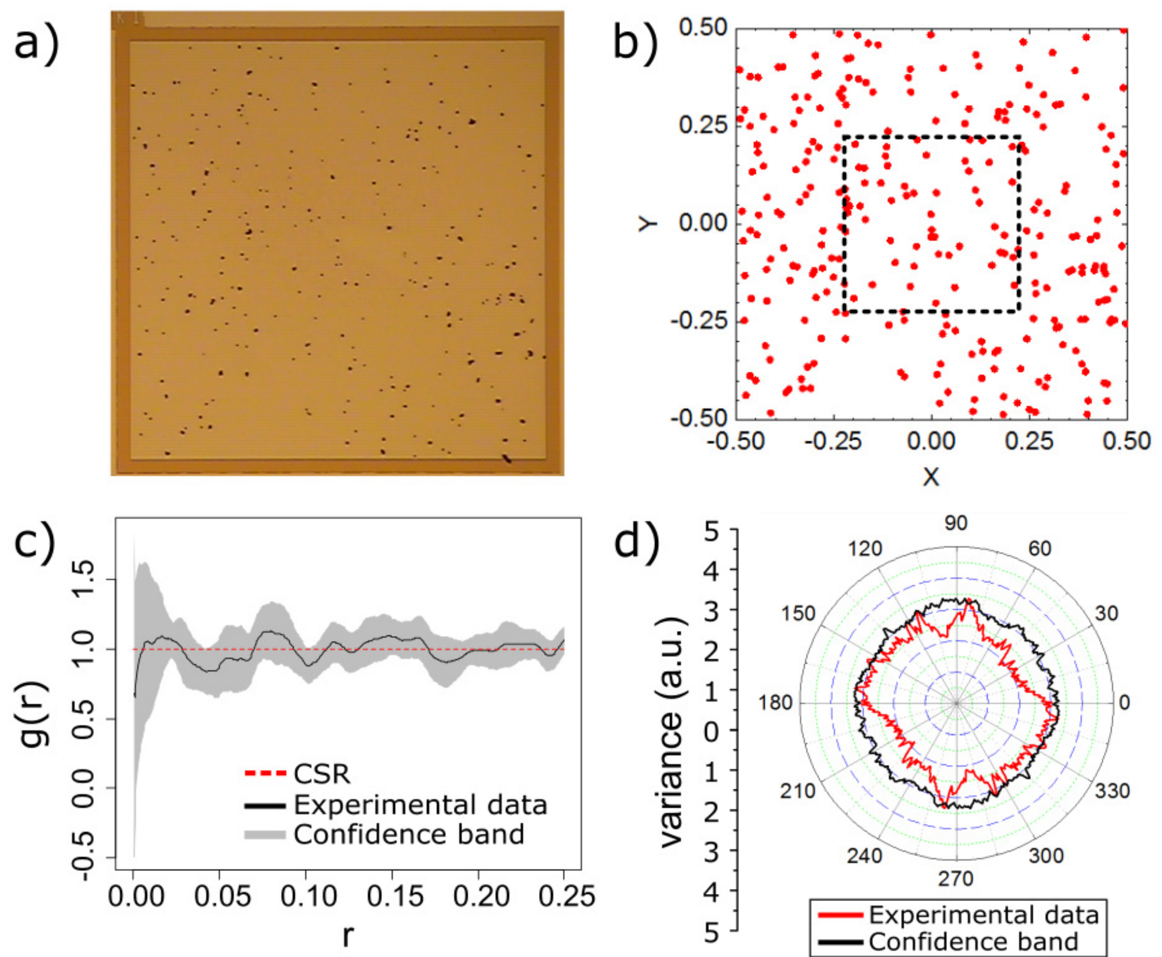

FIGURE 9

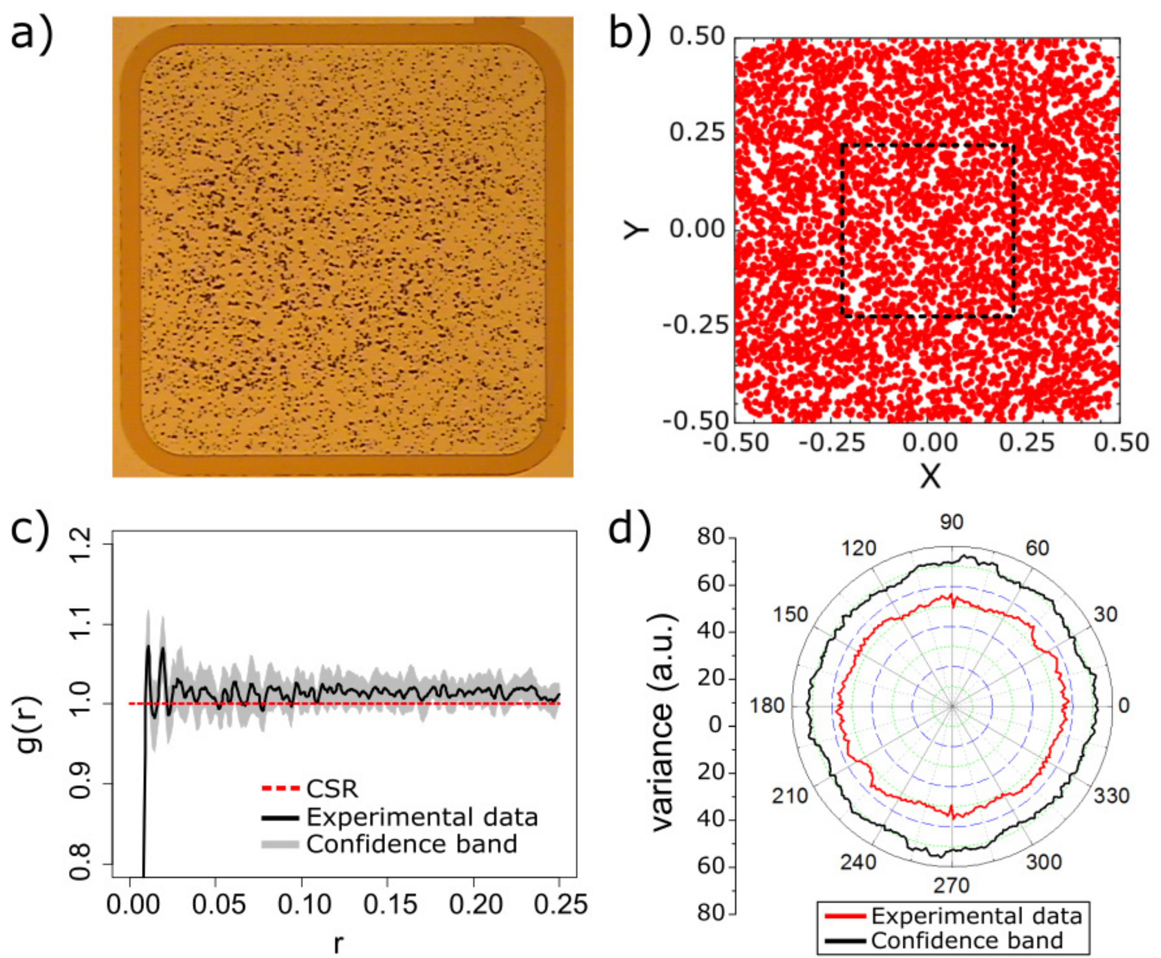

FIGURE 10

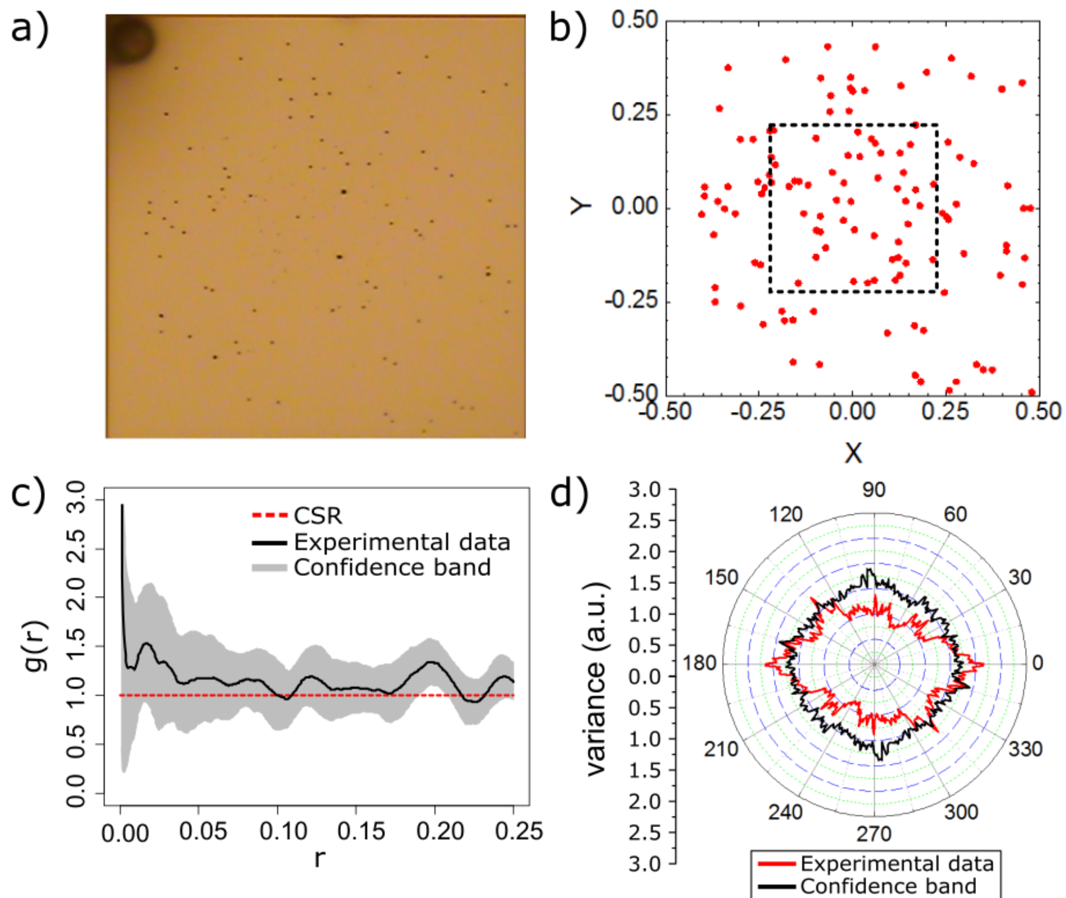

FIGURE 11

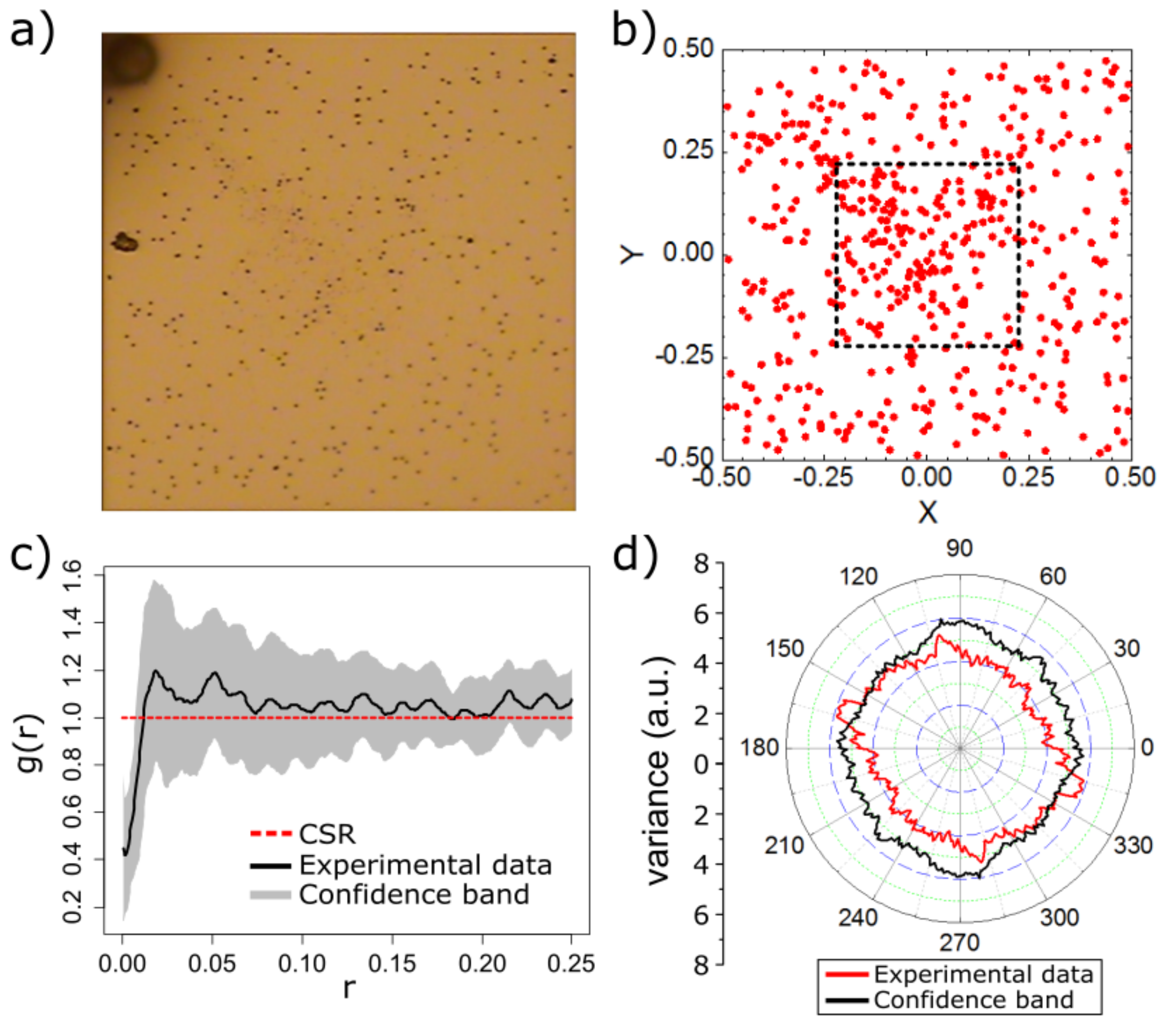

FIGURE 12

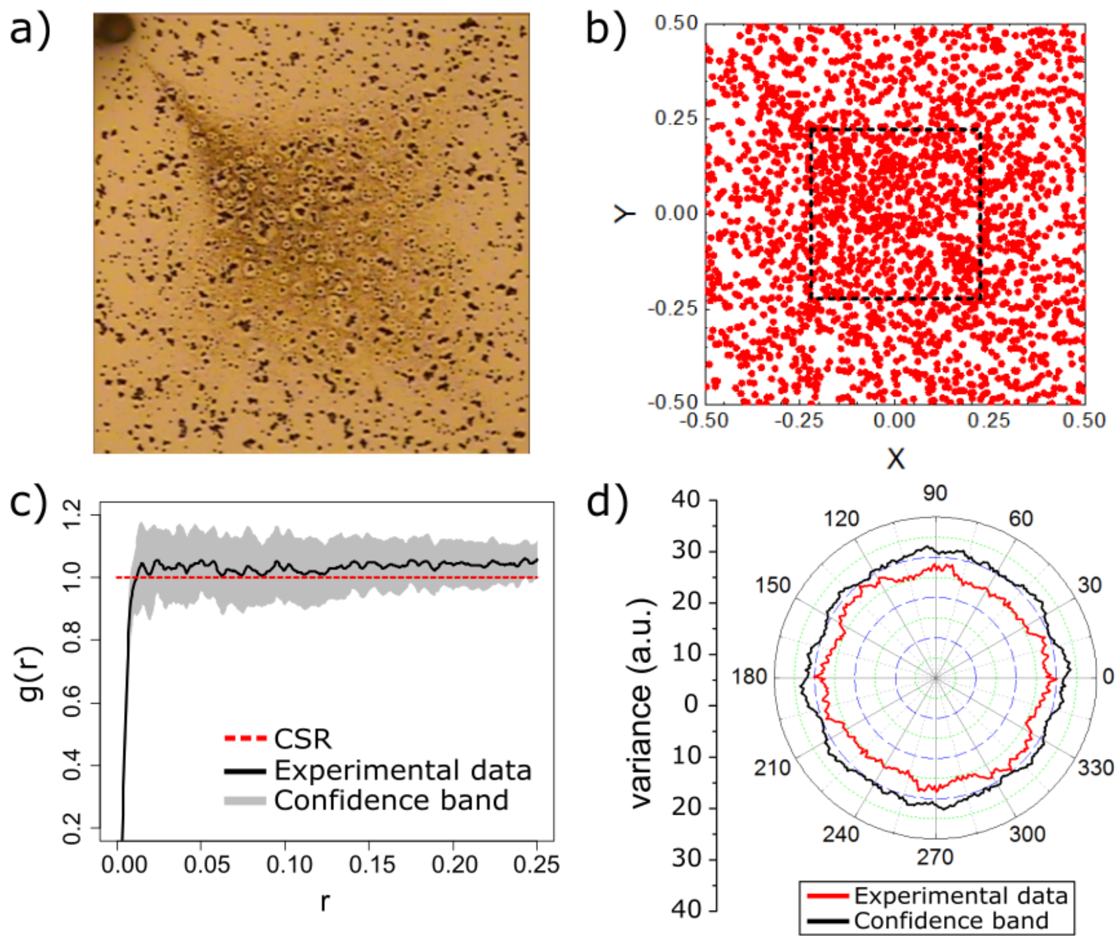

FIGURE 13

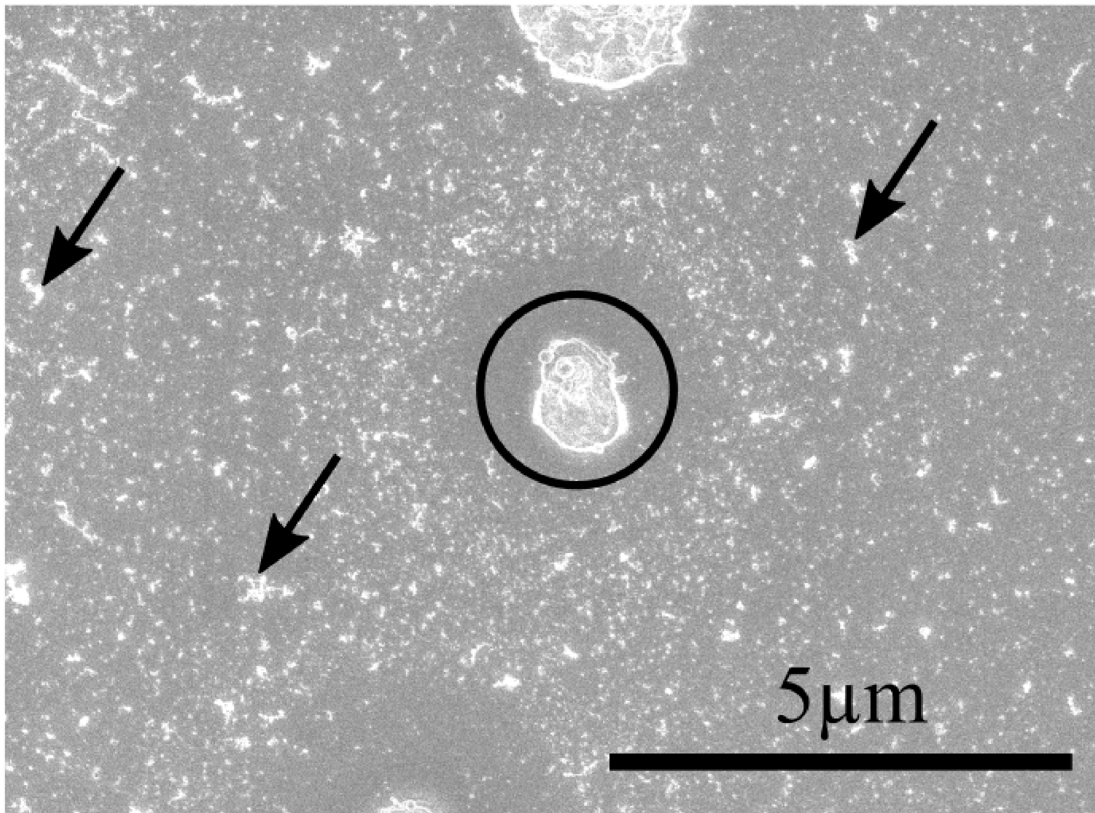

FIGURE 14

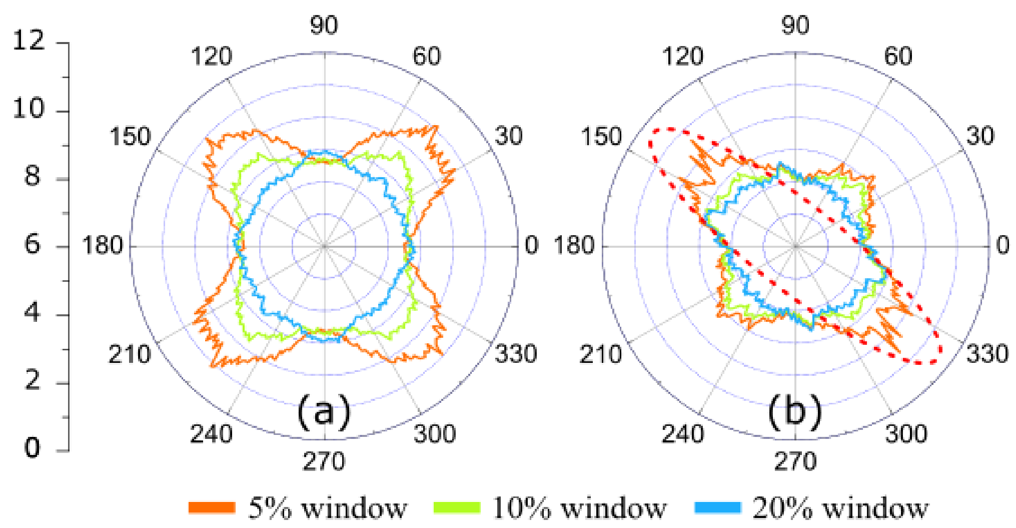

FIGURE 15

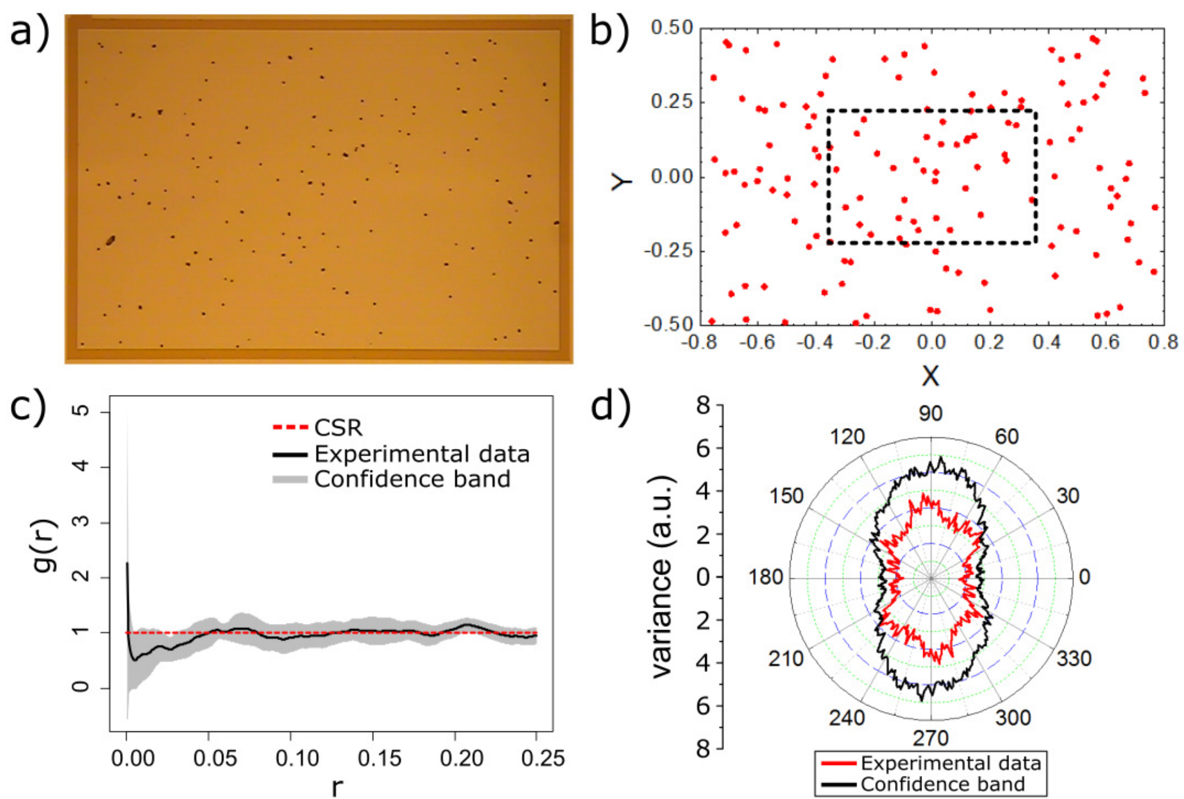

FIGURE 16

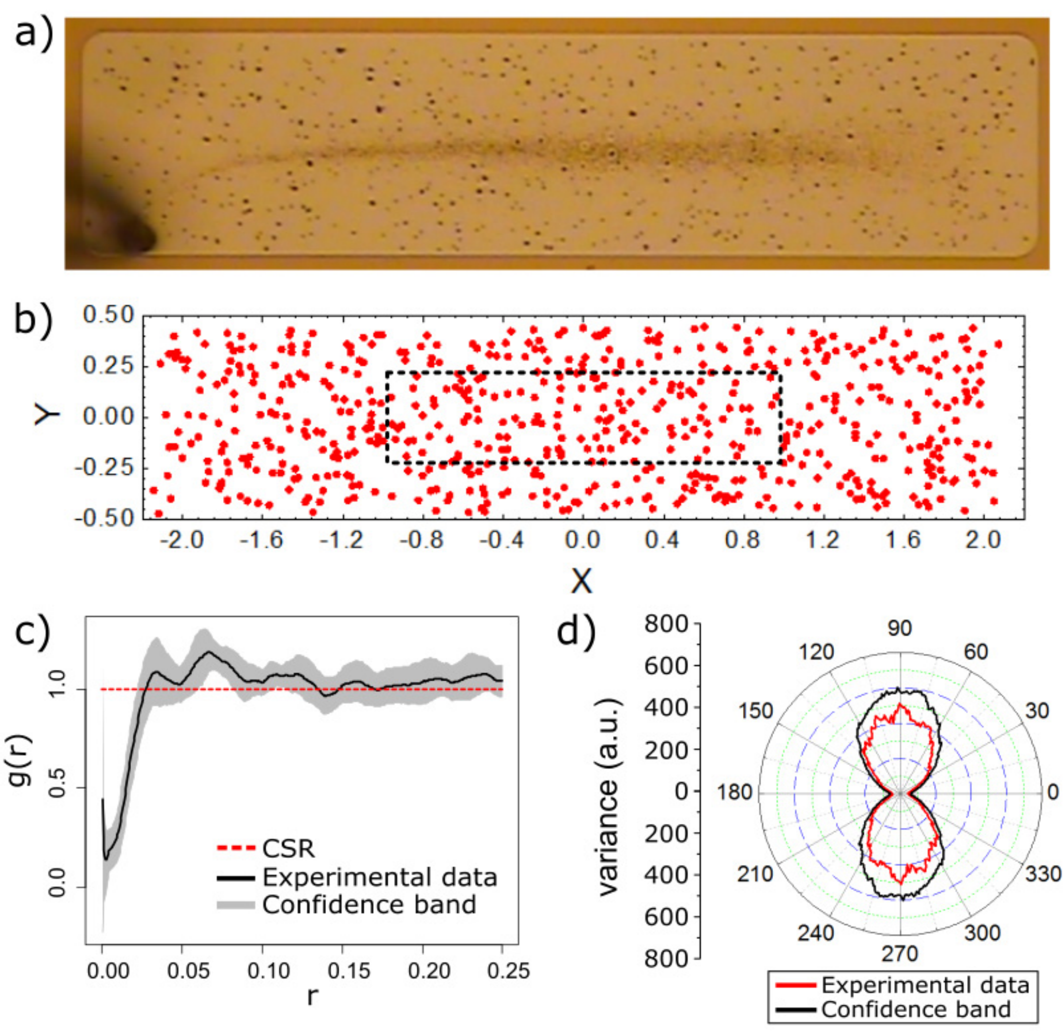

FIGURE 17